

## *Original*

Staron, P.; Fischer, T.; Eims, E.-H.; Froembgen, S.; Schell, N.; Daneshpour, S.;  
Martins, R.V.; Mueller, M.; Schreyer, A.:

### **Depth-resolved residual stress analysis with conical slits for highenergy X-rays**

Materials Science Forum, Mechanical Stress Evaluation by Neutrons  
and Synchrotron Radiation VI (2013)

Trans Tech Publications

DOI: [10.4028/www.scientific.net/MSF.772.3](https://doi.org/10.4028/www.scientific.net/MSF.772.3)

## Depth-resolved residual stress analysis with conical slits for high-energy X-rays

P. Staron<sup>1,a</sup>, T. Fischer<sup>1</sup>, E.-H. Eims<sup>1</sup>, S. Frömbgen<sup>1</sup>, N. Schell<sup>1</sup>,  
S. Daneshpour<sup>1</sup>, R.V. Martins<sup>2</sup>, M. Müller<sup>1</sup>, A. Schreyer<sup>1</sup>

<sup>1</sup>Institute of Materials Research, Helmholtz-Zentrum Geesthacht, 21502 Geesthacht, Germany

<sup>2</sup>Institute for Energy & Transport, European Commission, Joint Research Centre,  
1755 LE Petten, The Netherlands

<sup>a</sup>Peter.Staron@hzg.de

**Keywords:** high-energy X-rays; diffraction; conical slits; residual stress

**Abstract.** A conical slit cell for depth-resolved diffraction of high-energy X-rays was tested at the high-energy materials science beamline HEMS at PETRA III and used for the analysis of residual stresses in a laser beam welded steel overlap joint. With a conical slit width of 20  $\mu\text{m}$  and beam cross-sections below 100  $\mu\text{m}$ , depth resolutions well below 1 mm were achieved. The residual stress distributions obtained from the steel joint were in very good agreement with previous results from neutron diffraction measurements, although they were still noisier because of inferior grain statistics.

### Introduction

Currently, the most important diffraction techniques for spatially resolved non-destructive residual stress analysis in the interior of a sample are neutron diffraction (ND) and high-energy X-ray diffraction (HEXRD) using a white photon beam. Each technique has its specific advantages. The advantage of neutrons is that in most cases the wavelength can be chosen such that a scattering angle close to 90° can be used. This leads to a rectangular or cubic shape of the gauge volume, which is almost constant while rotating the sample for accessing different strain directions. The 90° scattering geometry can also have advantages when more complicated sample geometries are involved, like e.g. tubes. With the large penetration depth of neutrons for many materials, e.g. several centimetre thick steel plates can be analyzed.

The advantage of X-rays from a synchrotron source is the high intensity enabling high spatial resolution or fast measurements. The possibility of fast measurements can be used either for producing large two and three-dimensional strain maps or for *in situ* analyses of fast processes. Especially the white beam technique has been used for bulk as well as near-surface strain measurements [1, 2]. It enables recording a whole diffraction pattern in one shot, which can be used for determination of micro-stresses or for materials containing more than one phase.

In 1997, a conical slit cell (CSC) had been proposed for depth-resolved diffraction measurements with monochromatic high-energy X-ray beams [3]. The CSC has several concentric slits that are focussed on a spot within the sample by their conical shape [4]. With a CSC, complete diffraction rings can be measured with depth resolution, except for small regions where material is required for the mechanical stability of the slits. The analysis of full diffraction rings enables the simultaneous determination of all strain components in the plane. Moreover, also basic information on the texture of the material can be obtained. To achieve depth resolutions well below 1 mm, the slit width as well as the beam cross-section has to be around 20  $\mu\text{m}$  [5]. Thus, a third-generation synchrotron source with a high brilliance is required for their use. So far, only few examples for the application of CSC for residual stress and texture analysis can be found in the literature [6, 7, 8].

One CSC for cubic and one for hexagonal crystal structures were obtained from Institut für Mikrotechnik Mainz (IMM) and were tested at the new HZG beamline HEMS (High-Energy Materials Science) at the new PETRA III storage ring at DESY, Hamburg [9]. While depth resolutions of a few 100 micrometres can be achieved with narrow beams, the grain size of the

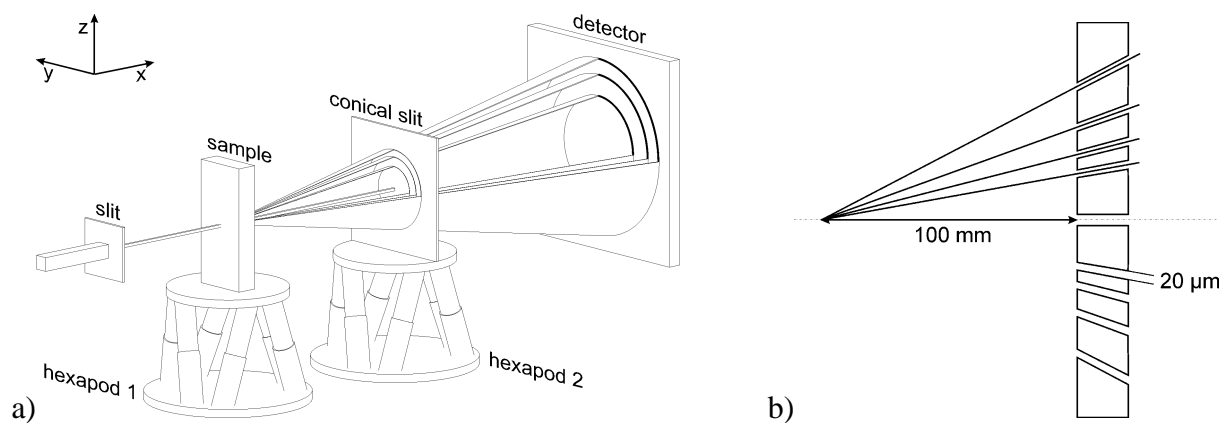


Fig. 1: Sketches of experimental setup (a) and conical slit geometry (b).

studied material often prevents a conventional analysis of diffraction rings with such high resolutions. However, in many cases only moderate depth resolutions are required, and with a larger beam cross section the grain statistics can be improved. The obtained results show that with a beam size of 50 μm and an energy resolution of 0.7% the depth resolution is about 0.7 mm.

The CSC was used for residual stress analysis in laser beam spot-welded steel overlap joints. Residual stresses can have a detrimental influence on the fatigue performance of welded material; thus, their knowledge is important for assessing material properties and performance. Since stress gradients along the depth of a weld are often important, the CSC can be used as a tool to study these stress distributions with high spatial resolution.

### Conical slits

**Geometry and adjustment.** The used CSC had seven conical slits with different radii that can be used for materials with cubic crystal structure. The width of the conical slits was 20 μm, the focus distance was 100 mm. The CSC was made of 2 mm thick Tungsten alloy. The ring radii were chosen such that a set of diffraction cones can pass the slits at a suitable photon energy (63.4 keV for Fe (Fig. 1)).

The CSC was mounted on a hexapod for easy adjustment (Fig. 1). In the first step, the centre of the conical ring slits has to be placed in the centre of the beam by shifting the CSC horizontally and vertically. In the second step, a thin sample is placed at the focus distance and the rotation of the CSC around  $y$  and  $z$ -axis is optimized. To avoid that the focal spot leaves the beam, the rotation axes are placed in the focal point. This is easily done with a hexapod by setting its pivot point. Finally, the position of the sample with respect to the gauge volume is determined precisely by scanning the sample in beam direction ( $x$ ) and using an area detector for recording the diffraction rings.

**Depth resolution.** The depth resolution is the most important parameter for the use of the CSC. It was measured for the (110) and (200) reflections by scanning a 0.5 mm thick pure Fe sample through the focus of the CSC. The intensity on the diffraction rings was integrated and plotted as a function of sample position. The full width at half maximum (FWHM) of the intensity curve was used to define the depth resolution (Table 1). The achieved depth resolution is between 0.7 and 1.4 mm for beam sizes between 50 and 150 μm. When several rings are used simultaneously it is important that the difference in the positions of the focal spots for these rings is small. For the two analyzed reflections the difference was 24 μm.

Below a beam size of 50 μm, the depth resolution did not decrease further. The reason is that the depth resolution is limited by the energy resolution given by the monochromator (double monochromator with elastically bent Si (111) crystals). Further improvement of depth resolution can be achieved with reduced energy resolution. Details can be learned, e.g., from a numerical simulation and will be published elsewhere.

beam width [ $\mu\text{m}$ ]	(110)		(200)	
	measured	deconv.	measured	deconv.
25	0.76	0.67	0.72	0.63
50	0.79	0.70	0.72	0.64
75	0.90	0.82	0.78	0.70
100	1.05	0.99	0.85	0.78
125	1.24	1.18	0.96	0.90
150	1.46	1.40	1.06	1.00

Table 1: Depth resolution in mm for different beam sizes and an energy resolution of 0.7%, measured with the Fe (110) and (200) reflections. The beam width is the edge length of the square beam cross-section. The measured values were deconvoluted with a step function representing the sample thickness.

### Residual stress in laser spot-welded steel sheets

**Material and weld.** Start and end points of laser welds are often prone to failure due to low penetration and imperfections or impurities as a result of keyhole collapse. Therefore, a new geometry had been developed for laser spot welds (LSW), where both start and end points are protected from external forces by a layer of continuously welded material [10]. This geometry was referred to as “pretzel” (Fig. 2). Fatigue tests have shown that the fatigue life of such laser beam welded overlap joints can significantly be improved with pretzel-type welds.

The laser weld was made at HZG using a 3.3 kW Nd:YAG laser. The welding speed was  $11 \text{ mm s}^{-1}$  and no shielding gas and filler wire were used for producing overlap welds. The material was deep-drawn DC04 steel, which is used in the automotive industry. The geometry of the overlap specimen is given in Fig. 2.

**Residual stresses.** Neutron diffraction had been used before for determining residual stresses (RS) in the two sheets of the overlap joints separately using a cubic gauge volume with a size of about 1.5 mm [10]. Residual strains had been determined in three orthogonal directions. The stress-free lattice parameter had been determined by assuming a plane stress state in the thin sheets. A modulus of elasticity of 225 GPa and a Poisson number of 0.28 had been used for calculating residual stresses for the (211) reflection. The results are shown as solid symbols in Fig. 3. They confirmed the validity of the used finite element model simulation [10]. However, the spatial resolution of 1.5 mm is probably insufficient to reveal details of the residual stress distribution in the complex weld geometry in lateral directions. Additionally, it is too large to analyze the intermediate layer between the two sheets, where fatigue cracks usually start under external load. Moreover, neutron exposure times are often too large to allow taking line scans with a large number of points with small gauge volumes or area scans for producing two-dimensional stress maps.

Here, high-energy synchrotron X-rays can contribute in a complementary manner because a large number of points can be measured within a short time, although not in three orthogonal directions. The X-ray results produced at a photon energy of 63.4 keV using the conical slits and a beam cross section of  $50 \mu\text{m} \times 50 \mu\text{m}$  are shown in Fig. 3 as small open symbols. The depth resolution was 0.7 mm (Table 1). A modulus of elasticity of 225 GPa and a Poisson number of 0.28

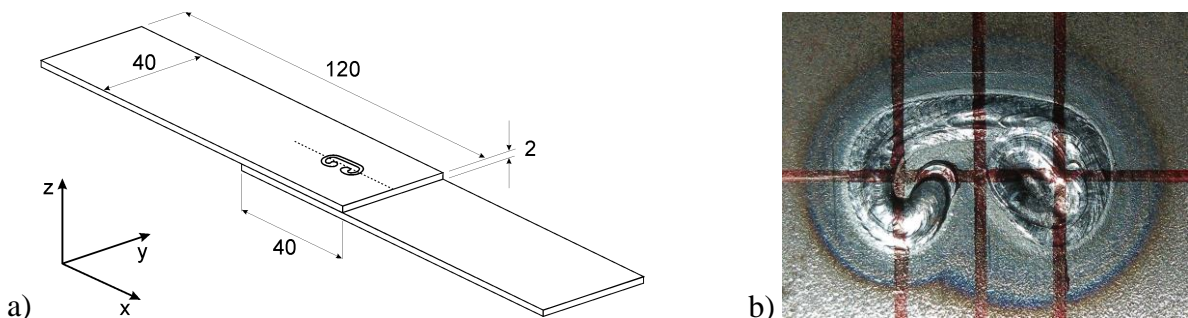


Fig. 2: a) Sketch of the laser welded joint. The dashed line indicates the scan line for strain measurements. b) Top view of the pretzel weld.

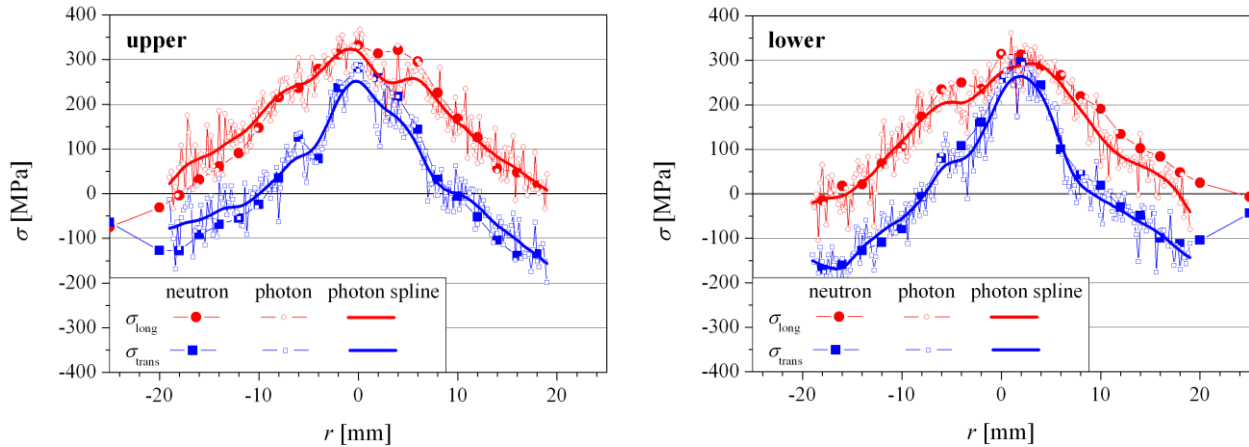


Fig. 3: RS in laser spot weld (pretzel-type), upper and lower sheet, along the line indicated in Fig. 2, neutron and X-ray results. The thick solid line is a spline function interpolating the noisy photon data.

were used for calculating residual stresses for the (110) reflection. The stress-free lattice parameter  $d_0$  was chosen such that the X-ray data match the neutron data. The X-ray data were interpolated by a spline function as a guide for the eye. The gauge volume size was a compromise between good depth resolution on the one hand, and sufficient intensity and grain statistics on the other hand. The results were still quite noisy, which was attributed to bad grain statistics. The mean grain size of the sample was  $26\ \mu\text{m}$  in the base material,  $15\ \mu\text{m}$  in the weld zone, and  $9\ \mu\text{m}$  in the heat-affected zone. The number of diffracting grains is small in this case not only because of the small beam size but also because of the small divergence of the beam coming from an undulator. To counteract that, the sample had already been shifted by 2 mm in  $y$ -direction (i.e. perpendicular to the scanning direction) during exposure to improve the grain statistics; but obviously, this had not been enough. Further significant improvement can be achieved by sample rotations during exposure. For this, the centre of rotation has to be within the centre of the gauge volume, which can again be achieved with a hexapod.

## Conclusions

Conical slits were used for depth-resolved residual stress analysis at a third-generation synchrotron source. The experimental set-up is relatively simple when a hexapod is used for the adjustment of the conical slit. With a conical slit size of  $20\ \mu\text{m}$  and a beam cross-section of  $50\ \mu\text{m} \times 50\ \mu\text{m}$  a depth resolution of 0.7 mm was achieved with a bent Si double monochromator with an energy resolution of 0.7%.

This opens up the possibility of depth-resolved residual stress analysis with monochromatic high-energy synchrotron X-rays. The depth resolution can be tuned with the beam cross-section from a few  $100\ \mu\text{m}$  to a few mm, depending on the energy resolution given by the monochromator. Since beam intensities are much higher than at neutron instruments, a large number of points can be measured within short time. Thus, two or three-dimensional stress maps can be produced, e.g. for comparison with predictions of finite element model simulations. However, the possibility of easy access to three orthogonal directions is missing. Moreover, in many cases measures have to be taken to improve the grain statistics. Consequently, neutrons and high-energy X-rays offer complementary capabilities.

## Acknowledgement

The authors are grateful to Petra Fischer from HZG for carrying out microstructural analyses on the laser beam spot-welded steel joint.

---

**References**

- [1] A. Pyzalla, *J. Nondestructive Evaluation* 19 (2000) 21–31.
- [2] C. Genzel, I.A. Denks, J. Gibmeier, M. Klaus, G. Wagener, *Nucl. Instr. Meth. Phys. Res. A* 578 (2007) 23–33.
- [3] H.F. Poulsen, S. Garbe, T. Lorentzen, D. Juul Jensen, F.W. Poulsen, N.H. Andersen, T. Frello, R. Feidenhansl, H. Graafsma, *J. Synchrotron Rad.* 4 (1997) 147–154.
- [4] S.F. Nielsen, A. Wolf, H.F. Poulsen, M. Ohler, U. Lienert, R.A. Owen, *J. Synchrotron Rad.* 7 (2000) 103–109.
- [5] R.V. Martins, Ph.D. thesis, Technical University of Berlin, 2002.
- [6] R.V. Martins, U. Lienert, L. Margulies, A. Pyzalla, *J. Neutron Research* 9 (2001) 249–254.
- [7] R.V. Martins, U. Lienert, L. Margulies, A. Pyzalla, *Mater. Sci. Forum* 404–407 (2002) 115–120.
- [8] R.V. Martins, U. Lienert, L. Margulies, A. Pyzalla, *Materials Science and Engineering A* 402 (2005) 278–287.
- [9] P. Staron, N. Schell, A. Haibel, F. Beckmann, T. Lippmann, L. Lottermoser, J. Herzen, T. Fischer, M. Koçak, A. Schreyer, *Mater. Sci. Forum* 638–642 (2010) 2470–2475.
- [10] P. Martinson, S. Daneshpour, M. Koçak, S. Riekehr, P. Staron, *Materials and Design* 30 (2009) 3351–3359.